

# PERFORMANCE ANALYSIS OF 2D AND 3D ANTENNA ARRAYS FOR SOURCE LOCALIZATION

*Dinh Thang Vu, Alexandre Renaux, Rémy Boyer and Sylvie Marcos*

Laboratory of Signals and Systems (L2S), University Paris-Sud XI, CNRS, SUPELEC  
3, rue Joliot Curie 91192 Gif-sur-Yvette Cedex, France  
phone: + (33)1 6985 1763, fax: + (33)1 6985 1765, email: {Vu,Renaux,Remy.Boyer,Marcos}@lss.supelec.fr

## ABSTRACT

In the context of passive sources localization using an antenna array, estimation performance in terms of elevation and azimuth is related to the kind of estimator used, and also to the geometry of the considered antenna array. Although there are several available results in the literature about linear and circular arrays, other possible geometries have been less studied. In this paper, we study the impact of the array geometry for two kinds of antenna arrays: the so called V-shaped antenna array (2D) and its 3D extension. The Cramér Rao lower Bound (CRB) will be used in this context as a useful tool to find the optimal configuration. The performance of the proposed antenna arrays is verified by comparing its CRB to the one of the standard uniform circular antenna from both analytical and simulation results.

## 1. INTRODUCTION

Direction of arrival (DOA) estimation of sources by an array of sensors has been widely studied in the array signal processing literature. The geometry of the array is one way to improve the parameters estimation performance and to avoid the ambiguities. A huge amount of results is available for linear and circular arrays (uniform or not) [1, 2]. More generally, planar (or 2D) arrays have also been studied. But the case of 3D arrays has surprisingly been less studied. However, there are several applications where the sensors are scattered in the 3D space. Consequently, the antenna has an arbitrary shape *e.g.* telescopes networks on the Earth's surface, electrodes networks on the skull of a patient, network of buoys on the sea's surface, etc.

Particularly, in [3] (chapter 4), the analysis of the antenna arrays through their diagrams of radiation pattern was presented. In a recent work [4], the ambiguity of the antenna arrays was studied by using differential geometry as a useful tool. There are also some works concerning the study of CRB in case of planar antenna arrays with non-standard geometry. We can cite here, for example, [5] and [6], where, contrary to our study, the sources are assumed random, hence leading to different expressions of the CRB and where the study is limited to the 2D antenna arrays. In this paper, we are interested to the impact of the array geometry in terms of estimation performance. Consequently, we use the CRB [7] as a benchmark to optimize the sensors position.

The antenna array structure proposed here is a first step for studying the 3D antenna. This allows us to compare our results with the works done in [5] and [8], on the so-called V-shaped antenna by measuring the contribution of the third di-

mension. Besides the fact that this type of network has been less studied in the literature, we adopt an approach where the two considered geometries have a degree of freedom, which is formed by the opening angle  $\Delta$  between the two branches located on the plane of each array. This explains why the studied antenna array is called V-shaped antenna in opposition to the more classical L-shaped antenna array (*i.e.*,  $\Delta = \frac{\pi}{2}$ ) [9]. As a result, the obtained CRB depends on this opening angle through the steering vector and allows us to study the optimization of the sensors positions. Several analytical and simulation results are given to prove that the 3D antenna overcomes the ambiguity problem of the 2D antenna. Moreover we show that there are some circumstances in which the 3D antenna has better estimation performance than the 2D antenna even for a weaker aperture.

The notational convention adopted in this paper is listed as follows: italic indicates a scalar quantity, bold minuscule indicates a vector, bold majuscule indicates a matrix.

The paper is organized as follows. In Sec. 2, the problem and the observation model are introduced. The analytic expressions of CRB for the V-shaped antenna arrays, and for its 3D extension are derived in Sec. 3. Finally, an analysis and some simulations concerning the analytic CRB are presented in Sec. 4.

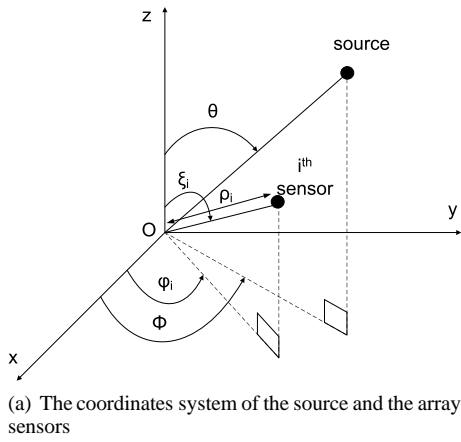
## 2. MODEL SETUP

We here consider the localization of a source emitting a deterministic and narrow band signal  $s(t)$  using an antenna array consisting of identical and omni-directional sensors. The positions in space of the source and the  $i^{\text{th}}$  sensors of the antenna array are given by their spherical coordinates, *i.e.*, the couple  $(\theta, \phi)$  for the source (assumed to be in the far field area) and the triplet  $(\rho_i, \varphi_i, \xi_i)$  for the  $i^{\text{th}}$  sensor (see Fig. 1(a)). In this study, we consider two geometries of antenna arrays. The first one concerns a planar V-shaped antenna array where its two branches, separated by an opening angle noted  $\Delta$ , consist of two linear not necessarily uniform antenna arrays. Note that the same analysis can be found in [5] for a Gaussian (unconditional) source. The second one is an extension of this planar array where a branch (also consisting of a linear array not necessarily uniform) orthogonal to the plane is added (see Fig. 1(b)). From the aforementioned assumptions, an analysis of the inter-sensors delay leads to the following observation model at the output of the antenna array [10]:

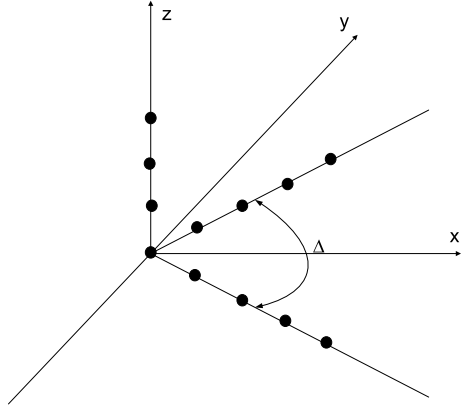
$$\mathbf{y}(t) = [y_1(t) \dots y_M(t)]^T = \mathbf{a}(\theta, \phi)s(t) + \mathbf{n}(t), \quad (1)$$

where  $t = 1, \dots, T$ , in which  $T$  denotes the number of snapshots,  $\lambda$  denotes the wavelength and  $\mathbf{a}(\theta, \phi)$  is the steering

This project is funded by both the Digiteo Research Park and the Région Île-de-France.



(a) The coordinates system of the source and the array sensors



(b) Geometry of the 3D antenna (In case of the 2D antenna, only the sensors located on the x0y plane are presented)

Figure 1: The geometry of the problem

vector given by:

$$\mathbf{a}(\theta, \phi) = \begin{bmatrix} e^{\frac{2j\pi\rho_1}{\lambda}(\sin\theta\sin\xi_1\cos(\phi-\phi_1)+\cos\xi_1\cos\theta)} \\ \vdots \\ e^{\frac{2j\pi\rho_M}{\lambda}(\sin\theta\sin\xi_M\cos(\phi-\phi_M)+\cos\xi_M\cos\theta)} \end{bmatrix}. \quad (2)$$

The number of sensors located on the plane is denoted by  $N_1$ , and the number of sensors located on the orthogonal branch in the case of a 3D antenna array is denoted by  $N_2$ . The total number of sensors  $M = N_1 + N_2$  will be constant for the comparison of these two arrays. The noise vector  $\mathbf{n}(t) \in \mathbb{C}^M$  is assumed to be Gaussian, circular, independent and identically distributed with zero-mean and covariance matrix  $\sigma^2\mathbf{I}$ .

### 3. CRAMÉR-RAO BOUND

The analysis of the ultimate performance, in terms of variance, that an unbiased estimator might achieve is generally conducted by using the CRB. In the case of the observation model (1), it is clear that  $\mathbf{y}(t)$  is distributed according to a multivariate Gaussian distribution with mean  $\mathbf{a}(\theta, \phi)s(t)$ , and variance  $\sigma^2\mathbf{I}$ . The parameters of interest in this study are the azimuth and the elevation, *i.e.*,  $\phi$  and  $\theta$  (since these parameters are decoupled from the noise variance, this latter

is omitted). We can notice that only the mean of  $\mathbf{y}(t)$  is parameterized. In this case, after the concatenation of all the observation vectors ( $t = 1, \dots, T$ ), the CRB, noted  $\mathbf{C}$ , can be deduced from [11] and [12]:

$$\mathbf{C} = \begin{bmatrix} C_{\theta\theta} & C_{\theta\phi} \\ C_{\phi\theta} & C_{\phi\phi} \end{bmatrix} = \frac{\sigma^2}{2s^H s} \begin{bmatrix} \text{Re} \left( \frac{\partial \mathbf{a}^H(\theta, \phi)}{\partial \theta} \frac{\partial \mathbf{a}(\theta, \phi)}{\partial \theta} \right) & \text{Re} \left( \frac{\partial \mathbf{a}^H(\theta, \phi)}{\partial \theta} \frac{\partial \mathbf{a}(\theta, \phi)}{\partial \phi} \right) \\ \text{Re} \left( \frac{\partial \mathbf{a}^H(\theta, \phi)}{\partial \phi} \frac{\partial \mathbf{a}(\theta, \phi)}{\partial \theta} \right) & \text{Re} \left( \frac{\partial \mathbf{a}^H(\theta, \phi)}{\partial \phi} \frac{\partial \mathbf{a}(\theta, \phi)}{\partial \phi} \right) \end{bmatrix}^{-1}, \quad (3)$$

where  $\mathbf{s} = [s(1) \dots s(T)]^T$  and, where  $C_{\theta\theta}$  and  $C_{\phi\phi}$  denote the CRB concerning the elevation and the azimuth, respectively, and  $C_{\theta\phi} = C_{\phi\theta}$  represent the coupling between the parameters  $\theta$  and  $\phi$ .

Thanks to the structure of the steering vector given by the observation model (1) and after some computational efforts detailed in the appendix, we obtain an analytic expression of the CRB for the 3D antenna array:

$$\begin{cases} C_{\theta\theta}^{3D} = \frac{2}{C_{SNR}} \frac{1 - \cos\Delta \cos 2\phi}{S_1 \sin^2 \Delta \cos^2 \theta + 2S_2 \sin^2 \theta (1 - \cos\Delta \cos 2\phi)}, \\ C_{\phi\phi}^{3D} = \frac{4}{C_{SNR} \sin^2 \theta} \frac{\frac{1}{2} S_1 \cos^2 \theta (1 + \cos\Delta \cos 2\phi) + S_2 \sin^2 \theta}{S_1^2 \sin^2 \Delta \cos^2 \theta + 2S_1 S_2 \sin^2 \theta (1 - \cos\Delta \cos 2\phi)}, \\ C_{\theta\phi}^{3D} = \frac{1}{C_{SNR} \tan \theta} \frac{S_1 \cos \Delta \sin 2\phi}{S_1^2 \sin^2 \Delta \cos^2 \theta + 2S_1 S_2 \sin^2 \theta (1 - \cos\Delta \cos 2\phi)}, \end{cases} \quad (4)$$

where, the following notations are adopted:  $\|\mathbf{s}\|^2 = s^H s$ ,  $C_{SNR} = \frac{8\pi^2 \|\mathbf{s}\|^2}{\sigma^2 \lambda^2}$ ,  $S_1 = \sum_{i=1}^{N_1} \rho_i^2$ , and  $S_2 = \sum_{i=N_1+1}^{N_1+N_2} \rho_i^2$  for  $N_2 \geq 1$ .

Since the 2D array is only a particular case of the 3D array ( $N_2 = 0$ ), the CRB are obtained by letting  $S_2 = 0$  in the above equations, leading to:

$$\begin{cases} C_{\theta\theta}^{2D} = \frac{2}{C_{SNR}} \frac{1 - \cos\Delta \cos 2\phi}{S_1 \sin^2 \Delta \cos^2 \theta}, \\ C_{\phi\phi}^{2D} = \frac{2}{C_{SNR}} \frac{1 + \cos\Delta \cos 2\phi}{S_1 \sin^2 \Delta \sin^2 \theta}, \\ C_{\theta\phi}^{2D} = \frac{1}{C_{SNR}} \frac{\cos \Delta \sin 2\phi}{S_1 \sin^2 \Delta \cos \theta \sin \theta}. \end{cases} \quad (5)$$

Moreover, in the particular case where  $\Delta = \frac{\pi}{2}$ , *i.e.*, when the 2D and 3D arrays represent the canonical basis of  $\mathbb{R}^2$  and of  $\mathbb{R}^3$ , respectively, we obtain the following more compact expressions:

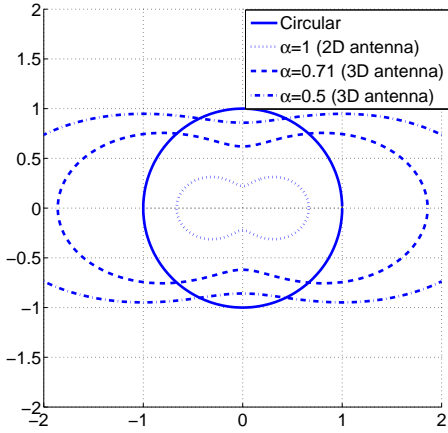
$$\begin{cases} C_{\theta\theta}^{3D\perp} = \frac{1}{C_{SNR}} \frac{2}{S_1 \cos^2 \theta + 2S_2 \sin^2 \theta}, \\ C_{\phi\phi}^{3D\perp} = \frac{2}{C_{SNR} S_1 \sin^2 \theta}, \\ C_{\theta\phi}^{3D\perp} = 0, \end{cases} \quad (6)$$

and

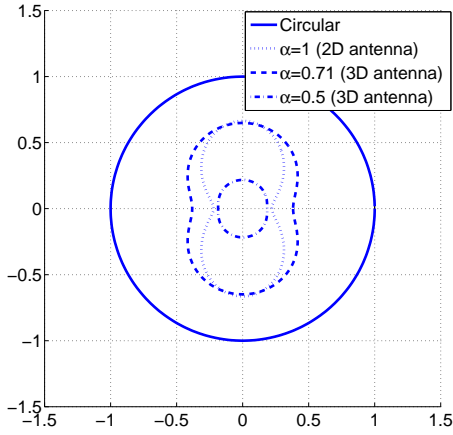
$$\begin{cases} C_{\theta\theta}^{2D\perp} = \frac{2}{C_{SNR} S_1 \cos^2 \theta}, \\ C_{\phi\phi}^{2D\perp} = \frac{2}{C_{SNR} S_1 \sin^2 \theta}, \\ C_{\theta\phi}^{2D\perp} = 0. \end{cases} \quad (7)$$

From these expressions, two important remarks can be done:

- When the source is located in the plane  $x0y$ , *i.e.*,  $\theta = \frac{\pi}{2}$ ,  $C_{\theta\theta}^{2D}$  tends to infinity, while  $C_{\theta\theta}^{3D}$  remains finite. Consequently, the 3D array overcomes the ambiguity problem of the 2D array.



(a)  $C_{\phi\phi}^{-1}/C_{\phi\phi}^{UCA}$  versus  $\phi$  with respect to  $\alpha$  for  $\Delta = 60^\circ$  and  $\theta = 45^\circ$



(b)  $C_{\theta\theta}^{-1}/C_{\theta\theta}^{UCA}$  versus  $\phi$  with respect to  $\alpha$  for  $\Delta = 60^\circ$  and  $\theta = 45^\circ$

Figure 2: Comparison of performance between V-shaped antenna and UCA

- In the case where  $\Delta = \frac{\pi}{2}$ ,  $\phi$  and  $\theta$  become decoupled, which confirms the intuition. Moreover,  $C_{\phi\phi}^{3D\perp}$  and  $C_{\phi\phi}^{2D\perp}$  no longer depend on  $\phi$  (isotropic property with respect to  $\phi$ ). Furthermore, if  $S_1 = 2S_2$ , *i.e.*, the three branches of the 3D array are made of a uniform linear array with the same number of sensors, the estimation concerning  $\theta$  no longer depends on the source's position (isotropic property with respect to both  $\theta$  and  $\phi$ ) in the case of the 3D array.

#### 4. ANALYSIS AND SIMULATIONS

In this section, the behavior of the CRB calculated in the previous section with respect to the degree of freedom  $\Delta$  is analyzed. We assume that, all branches, *i.e.* two branches for the 2D antenna, and three branches for the 3D antenna, are made from uniform linear arrays (ULA) with a half-wavelength inter-sensors spacing. All simulations are realized with a signal to noise ratio of 10dB and  $T = 50$  snapshots.

It is interesting to compare the performance of the V-

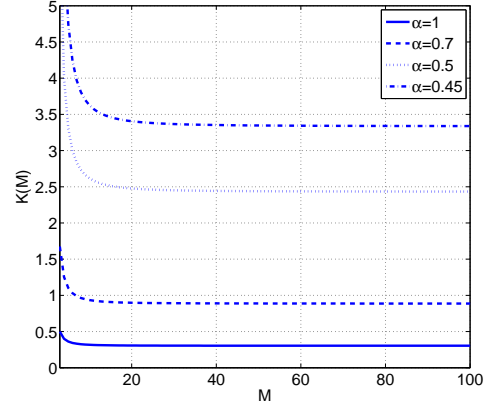


Figure 3:  $K(M)$  with respect to the number of sensors  $M$

shaped array with a classical isotropic planar array such that the uniform circular array (UCA). These arrays have the same number of sensors. The UCA having its sensors separated equidistantly with a half-wavelength spacing, its radius is given by [13]:  $r = \frac{\lambda}{4 \sin \frac{\Delta}{M}}$ . By letting  $\alpha = \frac{N}{M}$ , it is clear that the value of  $\alpha$  associated to the planar array is equal to 1, while the one associated to the 3D array is strictly lower than 1. The Fig. 2(a) and (b) represent, respectively, the CRB concerning the azimuth and elevation versus azimuth  $\phi$ , *w.r.t*  $\alpha$ , for the opening angle  $\Delta = 60^\circ$ , and the elevation  $\theta = 45^\circ$ . In order to compare the V-shaped antenna with the UCA, the bounds are normalized by the CRB of the UCA. One can observe that the estimation performance concerning elevation with a V-shaped array is always better than with a UCA, while the one concerning azimuth depends on the number of sensors located on the orthogonal branch, *i.e.*, on the coefficient  $\alpha$ . For a value of  $\alpha$  close to 1, the estimation concerning elevation with a V-shaped array is better than with an UCA.

In particular, we are interested to detail the performance comparison in the case where the V-shaped array and its 3D extension are isotropic ( $\Delta = \frac{\pi}{2}$ ). In this case, we just consider a comparison concerning the CRB of azimuth of these arrays. Let us consider

$$K(M) = \frac{3}{\alpha(\alpha^2 M^2 - 1) \sin^2 \frac{\pi}{M}}, \quad (8)$$

where  $K(M) = \frac{C_{\phi\phi}^{2D\perp}}{C_{\phi\phi}^{UCA}}$  if  $\alpha = 1$  and  $K(M) = \frac{C_{\phi\phi}^{3D\perp}}{C_{\phi\phi}^{UCA}}$  if  $\alpha < 1$ . It is clear that  $K(M) = \frac{3}{\pi^2}$  if  $\alpha = 1$  and  $M \gg 1$  or  $K(M) = \frac{3}{\pi^2 \alpha^3}$  if  $\alpha < 1$  and  $\alpha M \gg 1$ . We can say that the V-shaped array leads to better performance in terms of azimuth estimation than the UCA if and only if the ratio  $K(M)$  is lower than 1. Fig. 3 shows the behavior of  $K(M)$  with respect to the number of sensors  $M$  and to the coefficient  $\alpha$ .

Tab. 1 shows the value of  $1 - K(M)$  *w.r.t.*  $\alpha$  for a large number of sensors. This value represents the gain, concerning the azimuth estimation, of the V-shaped isotropic antenna array compared to the UCA antenna. We here want to find the value of  $\alpha$ , with which  $1 - K(M) > 0$  *i.e.*, the V-shaped antenna array has the better azimuth estimation accuracy than the UCA antenna. It is clear that, for all  $\alpha > 0.69$ , the 3D V-

Table 1: 'The azimuth estimation performance gain of 3D V-shaped isotropic antenna according to UCA'

$\alpha$	1	0.9	0.8	0.7	0.6
$1 - K(M)$	0.6959	0.5829	0.4060	0.1133	-0.4081

shaped isotropic array is always better than the UCA. Moreover, if  $\alpha = 1$  then the azimuth estimation accuracy of the 2D V-shaped isotropic planar array is nearly 70% better than the UCA antenna.

In the following, we compare the estimation performance between the 2D and 3D array. In this simulation, the 2D array is made from  $M = 7$  sensors (one at origin and three on each of the two branches). The 3D array is also made with  $M = 7$  sensors (one at the origin, and two on each of the three branches). It should be noted that taking some sensors from the planar array of the 2D antenna array to make the 3D antenna array will decrease the aperture and hence, reduce its performance. Therefore, using non ULA such as minimum redundancy [14], D-optimal [15], etc. instead of using ULA can maintain the aperture and also, the performance.

Fig. 4(a) shows the behavior of  $C_{\theta\theta}^{3D}$ ,  $C_{\theta\theta}^{2D}$ ,  $C_{\phi\phi}^{3D}$  and  $C_{\phi\phi}^{2D}$  with respect to the opening angle  $\Delta$  varying from 0 to  $\frac{\pi}{2}$ . For this simulation, the values of  $\phi$  and  $\theta$  are respectively  $20^\circ$  and  $70^\circ$ . In this scenario, the source is low according to the plane of the array. We observe that for the estimation of the elevation  $\theta$ , the 3D array always attains better performance than the 2D array. In this case, this is always true if the value of elevation satisfied  $\theta \geq 62.2^\circ$ , because, we can easily prove that

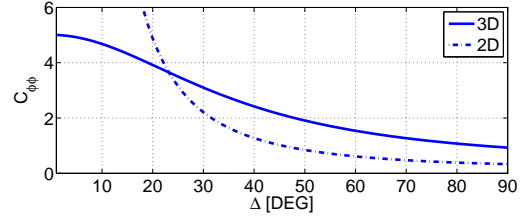
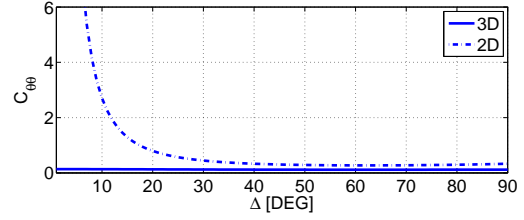
$$\frac{C_{\theta\theta}^{3D}}{C_{\theta\theta}^{2D}} < 1 \Leftrightarrow \theta > \arctan \sqrt{\max_{\Delta, \phi} \{\Gamma\}}. \quad (9)$$

where  $\Gamma = \frac{\sin^2 \Delta ((M^2 - 1) - \alpha(\alpha^2 M^2 - 1))}{(1 - \cos \Delta \cos 2\phi)^4 (1 - \alpha)((1 - \alpha)M + 1)(2(1 - \alpha)M + 1)}$ ,  $\alpha = \frac{N_1}{M} = \frac{5}{7}$ ,  $M = 7$ ,  $\theta \in [0^\circ, 90^\circ]$ ,  $\Delta \in (0^\circ, 180^\circ)$ ,  $\phi \in [0^\circ, 360^\circ]$ . On the contrary, there exists a value of  $\Delta$  (around  $23^\circ$  in this case), below which, the 3D array has better performance than the 2D array for the azimuth estimation. This critical value can be obtained by solving numerically the equation  $C_{\phi\phi}^{3D} = C_{\phi\phi}^{2D}$  with respect to  $\Delta$ .

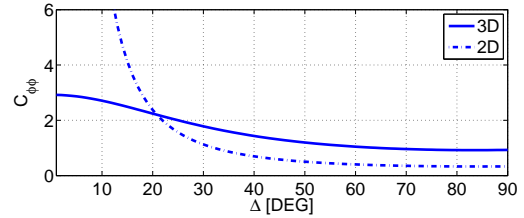
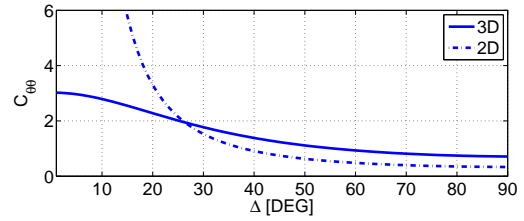
Fig. 4(b) shows the same curves, but for the value of  $\phi$  and  $\theta$  respectively equal to  $50^\circ$  and  $30^\circ$ . In this scenario, the source is high according to the plane of the array. In this case, we should, contrary to intuition, choose the 2D array over a certain limited of opening angle obtained by solving numerically  $\max(C_{\phi\phi}^{3D} = C_{\phi\phi}^{2D}, C_{\theta\theta}^{3D} = C_{\theta\theta}^{2D})$ .

## 5. CONCLUSION

In this paper the analytic expressions of CRB concerning azimuth and elevation of a single source under conditional observation model for both V-shaped array and its 3D extension is derived. Thanks to these results, an analysis of the two geometries is provided. We found that the 2D isotropic V-shaped array is always better than UCA in terms of estimation performance concerning azimuth. We also conclude that according to the source position in the space, below a certain value of the opening angle of the array, the V-shaped 3D ex-



(a) Behavior of  $C_{\theta\theta}^{3D}$ ,  $C_{\theta\theta}^{2D}$ ,  $C_{\phi\phi}^{3D}$  et  $C_{\phi\phi}^{2D}$  normalized by the CRB of UCA with respect to  $\Delta$  where  $\phi = 20^\circ$  and  $\theta = 70^\circ$



(b) Behavior of  $C_{\theta\theta}^{3D}$ ,  $C_{\theta\theta}^{2D}$ ,  $C_{\phi\phi}^{3D}$  et  $C_{\phi\phi}^{2D}$  normalized by the CRB of UCA with respect to  $\Delta$  where  $\phi = 50^\circ$  and  $\theta = 30^\circ$

Figure 4: Normalized CRB with respect to the opening angle  $\Delta$ .

tension array is always better than the V-shaped array for the same number of sensors with respect to estimation concerning azimuth or elevation. In contrast to this result, we show that there are values of  $\Delta$  such that the V-shaped array has better performance in terms of azimuth, while its 3D extension array obtains better performance in terms of elevation.

## 6. APPENDIX: PROOF OF (4)

The derivatives of the  $i^{th}$  element of the steering vector are given by:

$$\begin{aligned} \frac{\partial a_i(\theta, \phi)}{\partial \theta} &= \frac{2j\pi\rho_i}{\lambda} (\cos \theta \sin \xi_i \cos(\phi - \phi_i) - \cos \xi_i \sin \theta) \\ &\times e^{\left(\frac{2j\pi\rho_i}{\lambda} \sin \theta \sin \xi_i \cos(\phi - \phi_i) + \cos \xi_i \cos \theta\right)}, \\ \frac{\partial a_i(\theta, \phi)}{\partial \phi} &= -\frac{2j\pi\rho_i}{\lambda} \sin \theta \sin \xi_i \sin(\phi - \phi_i) \\ &\times e^{\left(\frac{2j\pi\rho_i}{\lambda} \sin \theta \sin \xi_i \cos(\phi - \phi_i) + \cos \xi_i \cos \theta\right)}. \end{aligned} \quad (10)$$

Let us assume that  $N_1$  is an odd number. Since the two branches of the V-shaped antenna are symmetric, then we have:

$$\begin{aligned} \sum_{i=1}^{N_1} \rho_i^2 e^{-2j\varphi_i} &= \sum_{i=1}^{\frac{N_1-1}{2}} \rho_i^2 e^{-2j\frac{\Delta}{2}} + \sum_{i=1}^{\frac{N_1-1}{2}} \rho_i^2 e^{2j\frac{\Delta}{2}} \\ &= \sum_{i=1}^{\frac{N_1-1}{2}} \rho_i^2 (e^{-j\Delta} + e^{j\Delta}) = 2 \cos \Delta \sum_{i=1}^{\frac{N_1-1}{2}} \rho_i^2 = S_1 \cos \Delta. \end{aligned} \quad (11)$$

It is clear that the parameter  $\xi_i = \frac{\pi}{2}$  for the sensors located on the plane  $xOy$  while  $\xi_i = 0$  for the sensors located on the orthogonal axis. Finally, applying (10) on (3) by using (11), the numerators of the CRB are given by:

$$\begin{aligned} \frac{[\mathbf{C}^{-1}]_{11}}{C_{SNR}} &= \sum_{i=1}^M \rho_i^2 (\cos \theta \sin \xi_i \cos(\phi - \varphi_i) - \cos \xi_i \sin \theta)^2 \\ &= \sum_{i=1}^{N_1} \rho_i^2 \cos^2 \theta \cos^2(\phi - \varphi_i) + \sum_{i=N_1+1}^M \rho_i^2 \sin^2 \theta \\ &= \frac{\cos^2 \theta}{4} \left( e^{2j\phi} \sum_{i=1}^{N_1} \rho_i^2 e^{-2j\varphi_i} + e^{-2j\phi} \sum_{i=1}^{N_1} \rho_i^2 e^{2j\varphi_i} \right. \\ &\quad \left. + 2 \sum_{i=1}^{N_1} \rho_i^2 \right) + \sin^2 \theta \sum_{i=N_1+1}^M \rho_i^2 \\ &= \frac{1}{4} \cos^2 \theta (S_1 \cos \Delta (e^{2j\phi} + e^{-2j\phi}) + 2S_1) + \sin^2 \theta S_2 \\ &= \frac{1}{2} S_1 \cos^2 \theta (\cos \Delta \cos 2\phi + 1) + S_2 \sin^2 \theta, \end{aligned} \quad (12)$$

$$\begin{aligned} \frac{[\mathbf{C}^{-1}]_{22}}{C_{SNR}} &= \sum_{i=1}^M \rho_i^2 (\sin \theta \sin \xi_i \sin(\phi - \varphi_i))^2 \\ &= \sin^2 \theta \sum_{i=1}^{N_1} \rho_i^2 \sin^2(\phi - \varphi_i) \\ &= -\frac{1}{4} \sin^2 \theta \left( e^{2j\phi} \sum_{i=1}^{N_1} \rho_i^2 e^{-2j\varphi_i} + e^{-2j\phi} \sum_{i=1}^{N_1} \rho_i^2 e^{2j\varphi_i} - 2 \sum_{i=1}^{N_1} \rho_i^2 \right) \\ &= -\frac{1}{4} \sin^2 \theta (S_1 \cos \Delta (e^{2j\phi} + e^{-2j\phi}) - 2S_1) \\ &= -\frac{1}{2} S_1 \sin^2 \theta (\cos \Delta \cos 2\phi - 1), \end{aligned} \quad (13)$$

and

$$\begin{aligned} \frac{[\mathbf{C}^{-1}]_{12}}{C_{SNR}} &= - \sum_{i=1}^M (\rho_i^2 \sin \theta \sin \xi_i \sin(\phi - \varphi_i) \\ &\quad \times (\cos \theta \sin \xi_i \cos(\phi - \varphi_i) - \cos \xi_i \sin \theta)) \\ &= - \sin \theta \cos \theta \sum_{i=1}^{N_1} \rho_i^2 \sin(\phi - \varphi_i) \cos(\phi - \varphi_i) \\ &= -\frac{1}{8j} \sin 2\theta \left( e^{2j\phi} \sum_{i=1}^{N_1} \rho_i^2 e^{-2j\varphi_i} - e^{-2j\phi} \sum_{i=1}^{N_1} \rho_i^2 e^{2j\varphi_i} \right) \\ &= -\frac{1}{8j} S_1 \sin 2\theta \cos \Delta (e^{2j\phi} - e^{-2j\phi}) \\ &= -\frac{1}{4} S_1 \sin 2\theta \cos \Delta \sin 2\phi. \end{aligned} \quad (14)$$

The denominator of CRB is given by:

$$\begin{aligned} \frac{\det[\mathbf{C}^{-1}]}{C_{SNR}^2} &= \frac{[\mathbf{C}^{-1}]_{11}[\mathbf{C}^{-1}]_{22} - [\mathbf{C}^{-1}]_{12}[\mathbf{C}^{-1}]_{21}}{C_{SNR}^2} \\ &= \left( \frac{1}{2} S_1 \cos^2 \theta (\cos \Delta \cos 2\phi + 1) + S_2 \sin^2 \theta \right) \\ &\quad \times \left( -\frac{1}{2} S_1 \sin^2 \theta (\cos \Delta \cos 2\phi - 1) \right) \\ &\quad - \left( \frac{1}{2} S_1 \sin \theta \cos \theta \cos \Delta \sin 2\phi \right)^2 \\ &= -\frac{1}{4} S_1^2 \sin^2 \theta \cos^2 \theta \cos^2 \Delta \cos^2 2\phi \\ &\quad + \frac{1}{4} S_1^2 \sin^2 \theta \cos^2 \theta - \frac{1}{2} S_1 S_2 \sin^4 \theta (\cos \Delta \cos 2\phi - 1) \\ &\quad - \frac{1}{4} S_1^2 \sin^2 \theta \cos^2 \theta \cos^2 \Delta \sin^2 2\phi \\ &= \frac{\sin^2 \theta}{4} (S_1^2 \cos^2 \theta \sin^2 \Delta + 2S_1 S_2 \sin^2 \theta (1 - \cos \Delta \cos 2\phi)). \end{aligned} \quad (15)$$

## REFERENCES

- [1] K. M. Reddy and V. U. Reddy, "Analysis of spatial smoothing with uniform circular arrays," *IEEE Trans. Signal Processing*, vol. 47, no. 6, pp. 1726–1730, Jun. 1999.
- [2] A. Tewfik and W. Hong, "On the application of uniform linear array bearing estimation techniques to uniform circular arrays," *IEEE Trans. Signal Processing*, vol. 40, no. 4, pp. 1008–1011, Apr. 1992.
- [3] H. L. VanTrees, *Detection, Estimation and Modulation Theory: Optimum Array Processing*. New York: Wiley, 2002, vol. 4.
- [4] A. Manikas, *Differential Geometry in Array Processing*. Imperial College Press, 2004.
- [5] H. Gazzah and S. Marcos, "Cramer Rao bounds for antenna array design," *IEEE Trans. Signal Processing*, vol. 54, no. 1, pp. 336–345, Jan. 2006.
- [6] A. Mirkin and L. H. Sibul, "Cramér-Rao bounds on angle estimation with a two-dimensional array," *IEEE Trans. Signal Processing*, vol. 39, pp. 515–517, Feb. 1991.
- [7] H. Cramér, *Mathematical Methods of Statistics*. New York: Princeton University, Press, 1946.
- [8] T. Filik and T. E. Tuncer, "Uniform and nonuniform V-shaped isotropic planar arrays," in *Proc. Sensor Array and Multichannel Signal Processing Workshop*, Darmstadt, Germany, Jul. 2008, pp. 99–103.
- [9] Y. Hua, T. K. Sarkar, and D. D. Weiner, "An L-shaped array for estimating 2D directions of wave arrival," *IEEE Trans. Antennas Propagat.*, vol. 39, pp. 143–146, Feb. 1991.
- [10] E. L. Lehmann, *Theory of Point Estimation*. New York: Wiley, 1983.
- [11] S. M. Kay, *Fundamentals of Statistical Signal Processing*. NJ: Prentice Hall, 1993, vol. 1.
- [12] A. V. D. Bos, "A Cramer Rao lower bound for complex parameters," *IEEE Trans. Acoust., Speech, Signal Processing*, vol. 42, p. 2859, Oct. 1994.
- [13] S. C. Chan and H. H. Chen, "Uniform concentric circular arrays with Frequency-Invariant Characteristics-Theory design, adaptive Beamforming and DOA estimation," *IEEE Trans. Signal Processing*, vol. 55, no. 1, pp. 165–177, Jan. 2007.
- [14] A. T. Moffet, "Minimum redundancy linear arrays," *IEEE Trans. Antennas Propagat.*, vol. 16, pp. 172–175, Mar. 1968.
- [15] X. Huang, J. P. Reilly, and M. Wong, "Optimal design of linear array of sensors," in *Proc. IEEE Int. Conf. Acoust., Speech, Signal Processing*, vol. 2, Toronto, Ont., Canada, May 1991, pp. 1405–1408.